

Data-Driven ART Counseling: Integrating Oocyte Quality Assessment with Personalized Cycle Predictions

David H. Silver^{1*}, Gilad Rave¹, Taher Odeh¹, Riska Fadilla¹

^{1*}Rhea Labs, Rhea Fertility, Singapore, Singapore.

*Corresponding author(s). E-mail(s): david.silver@rhea-fertility.com;

Contributing authors: gilad.rave@rhea-fertility.com;

taher@rhea-fertility.com; riska.fadilla@rhea-fertility.com;

Abstract

Assisted reproductive technology (ART) counseling traditionally relies on population-based statistics that inadequately capture individual patient variability in both cycle outcomes and oocyte quality assessment. We present a dual-model framework combining comprehensive parametric cycle simulation with data-driven oocyte quality evaluation to enable personalized IVF counseling. Our parametric calculator implements complete IVF cycle prediction from oocyte retrieval through live birth, incorporating age-dependent AMH percentiles, optional antral follicle count data, stage-specific attrition rates, and patient-specific factors (BMI, ethnicity, health conditions) through established clinical relationships. For oocyte quality assessment, we develop a Vision Transformer model using the publicly available time-lapse embryo dataset (Gomez et al., 2022), analyzing 702 post-ICSI oocyte images (acquired before pronuclear formation, pre-2PN) from standardized EmbryoScope™ acquisitions with blastulation outcomes to predict developmental potential. The parametric calculator demonstrates transparent relationships throughout the complete IVF process with multi-cycle projections and cumulative success probabilities. The oocyte quality assessment model achieves moderate but clinically meaningful correlation ($r = 0.421$) with actual blastulation outcomes and 71.1% classification accuracy with high sensitivity (97.6%) for identifying successful developmental candidates. This integrated framework provides clinicians with comprehensive, interpretable tools for evidence-based patient counseling while acknowledging realistic performance limitations suitable for clinical implementation.

Keywords: ART counseling, oocyte quality assessment, Vision Transformer, parametric modeling, reproductive medicine, artificial intelligence, ICSI, blastulation prediction

1 Introduction

Assisted reproductive technology (ART) represents a critical intervention for couples facing infertility and individuals seeking fertility preservation [Human Fertilisation and Embryology Authority \(2024\)](#); [Society for Assisted Reproductive Technology \(2024\)](#), yet current counseling approaches rely heavily on population-based statistics that inadequately capture individual patient variability [Gameiro et al. \(2023\)](#). Traditional protocols provide aggregate success rates stratified by broad demographics, failing to account for patient-specific factors such as age-dependent ovarian reserve markers and individual oocyte quality characteristics [Practice Committee of the American Society for Reproductive Medicine \(2017\)](#).

Current limitations are particularly evident in cycle outcome prediction and oocyte quality assessment. For predictions, clinicians often rely on simplified age-based estimates that ignore substantial individual variation in anti-Müllerian hormone (AMH) levels [Seifer et al. \(2002\)](#); [Practice Committee of the American Society for Reproductive Medicine \(2020\)](#). The dramatic age-dependent changes in AMH percentiles—declining from ~ 1.8 ng/mL at age 25 to ~ 0.18 ng/mL at age 42—are rarely considered in counseling protocols, leading to misleading patient prognoses [Lee et al. \(2017\)](#); [Song et al. \(2021\)](#).

For oocyte assessment, current practice relies on subjective morphological evaluation with significant inter-observer variability and limited predictive accuracy [Paternot et al. \(2009, 2011\)](#); [Fordham et al. \(2022\)](#). Even experienced embryologists show only moderate agreement when assessing blastocyst implantation probability, with artificial intelligence models often outperforming human assessment [Fordham et al. \(2022\)](#). This reactive approach limits opportunities for personalized treatment optimization [Racowsky et al. \(2010\)](#).

Recent advances in artificial intelligence offer promising solutions through Vision Transformer (ViT) models that have demonstrated remarkable capabilities in medical image analysis [Dosovitskiy et al. \(2021\)](#); [Al-hammuri et al. \(2023\)](#), while parametric modeling can incorporate established clinical relationships in transparent frameworks [Rudin \(2019\)](#). Previous work has shown algorithmic approaches can significantly enhance predictive accuracy in embryo assessment [Rave et al. \(2024\)](#), demonstrating clinical potential for AI-assisted reproductive medicine. The broader adoption of "deep technology" solutions across IVF laboratories—including automated cryostorage systems, digital inventory management, and integrated data analytics—reflects the field's commitment to technological advancement [Go and Hudson \(2023\)](#).

We present a comprehensive dual-model framework addressing both challenges through: (1) a parametric calculator incorporating age-dependent AMH percentiles and established clinical relationships for transparent oocyte retrieval predictions, and

(2) a Vision Transformer model trained on post-ICSI oocyte images to assess individual quality and predict blastulation outcomes.

This framework provides clinicians with evidence-based tools for personalized IVF counseling while maintaining realistic performance expectations [American Society for Reproductive Medicine Practice Committee \(2021\)](#). Our approach exemplifies responsible AI development, prioritizing transparency and honest performance reporting over unrealistic accuracy claims [Varoquaux and Cheplygina \(2022\)](#), demonstrating meaningful improvements over current subjective methods through rigorous validation and uncertainty quantification.

2 Methods

2.1 Dataset and Study Design

This study utilized the publicly available time-lapse embryo dataset by Gomez et al. [Gomez et al. \(2022\)](#), comprising 704 time-lapse videos with 2.4M images across 7 focal planes. We extracted 702 embryo samples with complete blastulation outcome data. Each sample included continuous quality scores (range: 0.004-0.999, mean: 0.592 ± 0.287) and binary blastulation labels ((66.7%) successful outcomes) [Awadalla et al. \(2021\)](#); [Zhu et al. \(2024\)](#). The dataset represents clinical variability from ICSI cycles (2011-2019, University Hospital of Nantes) with embryos cultured using standardized protocols and monitored via EmbryoScope™ time-lapse imaging systems.

Cross-validation used 8-fold stratified sampling to maintain class balance [Hastie et al. \(2009\)](#).

2.2 Parametric Cycle Prediction Calculator

The parametric calculator incorporates established clinical relationships through transparent mathematical models [Rudin \(2019\)](#).

2.2.1 Age-Dependent AMH Modeling

The calculator implements age-specific AMH percentile distributions [Lee et al. \(2017\)](#); [Song et al. \(2021\)](#):

$$\text{AMH}_{\text{normal}}(\text{age}) = f(\text{age-specific percentiles}) \quad (1)$$

where f represents a sigmoid function parametrized from published age-stratified AMH distributions [Lee et al. \(2017\)](#). The function captures AMH decline: median values decrease from ≈ 1.8 ng/mL at age 25 to ≈ 0.18 ng/mL at age 42, with 10th and 90th percentiles showing parallel patterns [Lee et al. \(2017\)](#).

2.2.2 IVF Cycle Prediction Pipeline

The parametric model implements complete IVF cycle simulation from oocyte retrieval through live birth, incorporating stage-specific attrition rates and patient-specific factors [Seifer et al. \(2002\)](#); [Practice Committee of the American Society for Reproductive Medicine \(2020\)](#).

Oocyte Retrieval Prediction: Oocyte yield combines age effects, AMH adjustments, and optional antral follicle count (AFC) data:

$$\text{Retrieved Oocytes} = \text{Base}(\text{age}) \times \text{AMH Factor}(\text{AMH}, \text{age}) \times \text{Health Factors} \quad (2)$$

The age-dependent baseline utilizes a sigmoid function to capture nonlinear decline in ovarian response [American College of Obstetricians and Gynecologists \(2017\)](#):

$$\text{Base}(\text{age}) = \text{sigmoid}(\text{age}, \text{age-specific parameters}) \quad (3)$$

The AMH factor employs a Gompertz growth function:

$$\text{AMH Factor} = \text{Gompertz} \left(\frac{\text{AMH}_{\text{patient}}}{\text{AMH}_{\text{normal}}(\text{age})} \right) \quad (4)$$

When AFC data is available, the model incorporates the Ovarian Response Prediction Index (ORPI):

$$\text{ORPI} = \frac{\text{AMH} \times \text{AFC}}{\text{age}} \quad (5)$$

Attrition Pipeline: The model simulates the full IVF process through age-stratified attrition rates:

$$\text{Frozen} = f_{\text{freeze}}(\text{Retrieved}, \text{age}, \text{ORPI}) \quad (6)$$

$$\text{Thawed} = \text{Frozen} \times \alpha_{\text{thaw}}(\text{age}) \quad (7)$$

$$\text{Fertilized} = \text{Thawed} \times \alpha_{\text{fert}}(\text{age}) \quad (8)$$

$$\text{Good Embryos} = \text{Fertilized} \times \alpha_{\text{embryo}}(\text{age}) \quad (9)$$

$$\text{Implanted} = \text{Good Embryos} \times \alpha_{\text{implant}}(\text{age}) \times \text{Patient Factors} \quad (10)$$

$$\text{Live Birth} = \text{Implanted} \times \alpha_{\text{birth}} \quad (11)$$

where $\alpha_{\text{stage}}(\text{age})$ represents age-specific attrition rates derived from clinical outcomes, and Patient Factors incorporate BMI effects (polynomial function), ethnicity adjustments, and health condition modifiers (e.g., PCOS enhances oocyte yield by (20%), endometriosis reduces implantation by (20%)) [Lee et al. \(2017\)](#).

Multiple Cycle Projections: The framework provides predictions for up to three consecutive cycles, accounting for age progression and cumulative live birth probabilities using probability theory for independent trials with age-dependent success rates.

2.3 Oocyte Quality Assessment Model

2.3.1 Vision Transformer Architecture

We implemented a Vision Transformer (ViT) model for oocyte quality assessment [Dosovitskiy et al. \(2021\)](#); [Al-hammuri et al. \(2023\)](#). The model processes

standardized post-ICSI oocyte images (224×224 pixels, acquired immediately after intracytoplasmic sperm injection but before pronuclear formation) through attention mechanisms that capture morphological features relevant to blastulation potential [Zhang et al. \(2021\)](#).

The ViT architecture consists of:

- Patch embedding layers (16×16 patches) for image tokenization into 196 patches
- 12-layer transformer with multi-head self-attention mechanisms (12 heads)
- Position encoding for spatial relationship preservation
- MLP classification head with dropout (0.1) for blastulation prediction
- Model parameters: ViT-Base/16 configuration with 86M parameters

Image Acquisition Protocol: Post-ICSI oocyte images were acquired using the EmbryoScopeTM time-lapse incubator system (Vitrolife©, Sweden) with a camera under a 635 nm LED light source passing through Hoffman’s contrast modulation optics [Gomez et al. \(2022\)](#). Images were captured every 10-20 minutes from fertilization through blastocyst development, with analysis focusing on post-ICSI, pre-2PN time-points. Images were normalized for brightness and contrast, then resized to 224×224 pixels while maintaining aspect ratio through center cropping.

2.3.2 Training and Validation

Model training utilized the complete 702-sample dataset with 8-fold cross-validation [Varoquaux and Cheplygina \(2022\)](#). Each fold maintained stratified sampling to preserve the (66.7%) positive class distribution.

Training parameters:

Parameter	Value
Optimizer	AdamW
Initial Learning Rate	3e-4
Weight Decay	0.01
Beta Values	(0.9, 0.999)
Batch Size	16
Max Epochs	100
Learning Rate Schedule	Cosine annealing with warm-up (5 epochs)
Early Stopping Patience	10 epochs
Early Stopping Metric	Validation AUC
Minimum Delta	0.001
Dropout Rate	0.1
Data Augmentation	Random horizontal flip (p=0.5), rotation ($\pm 15^\circ$)
Normalization	Z-score (channel-wise)

2.3.3 Performance Evaluation

Model performance was assessed using multiple metrics [Litjens et al. \(2017\)](#):

Continuous Prediction Metrics:

- Pearson correlation coefficient (r)
- Mean Absolute Error (MAE)

- Root Mean Square Error (RMSE)

Binary Classification Metrics:

- Accuracy, Precision, Recall, F1-Score
- Area Under the ROC Curve (AUC)
- Sensitivity and Specificity
- Positive and Negative Predictive Values

Statistical Validation: Cross-validation error bars were computed across all folds to quantify model stability. Statistical significance testing used Mann-Whitney U tests [Mann and Whitney \(1947\)](#) comparing model performance against baselines: (1) label-shuffled controls, (2) majority class classifier, and (3) random prediction baseline. Effect size calculations used Cohen’s d [Cohen \(1988\)](#).

Baseline Comparisons:

- **Random Classifier:** AUC = 0.500, accuracy = (50%)
- **Majority Class:** Always predicts positive class ((66.7%) accuracy)
- **Label Shuffle:** Same model architecture trained on randomized labels
- **Morphological Scoring:** Traditional embryologist assessment metrics

2.4 Integrated Framework Implementation

The dual-model framework provides clinical integration [Food and Drug Administration \(2022\)](#):

1. **Parametric Calculator Interface:** Web-based tool allowing clinicians to input patient age and AMH values for immediate oocyte yield predictions.
2. **Quality Assessment Pipeline:** Automated processing of oocyte images through the trained ViT model, providing quality scores and blastulation probability estimates.
3. **Combined Reporting:** Integrated output combining cycle predictions with individual oocyte quality assessments for comprehensive patient counseling [American Society for Reproductive Medicine Practice Committee \(2021\)](#).

All implementations prioritized transparency and clinical interpretability [Topol \(2019\)](#), ensuring predictions could be meaningfully discussed with patients and incorporated into clinical decision-making [Beauchamp and Childress \(2019\)](#).

3 Results

3.1 Dataset Characteristics

Analysis utilized 702 real embryo samples with quality scores ranging from 0.004 to 0.999 (mean: 0.592 ± 0.287). Binary classification distribution showed (66.7%) positive blastulation outcomes (468 successful, 234 unsuccessful), reflecting typical clinical IVF success rates.

3.2 Parametric Cycle Prediction Calculator Performance

The parametric calculator demonstrated comprehensive IVF cycle simulation capabilities, providing transparent relationships between patient-specific factors and predicted outcomes throughout the entire treatment process.

3.2.1 AMH-Based Predictions

Figure 1 illustrates oocyte yield predictions across AMH levels and age groups. The model captures expected relationships where higher AMH values consistently predict better retrieval outcomes, with effects most pronounced in younger patients. The visualization emphasizes age-dependent AMH interpretation through annotations clarifying effects "at any given age" and "at any given AMH level."

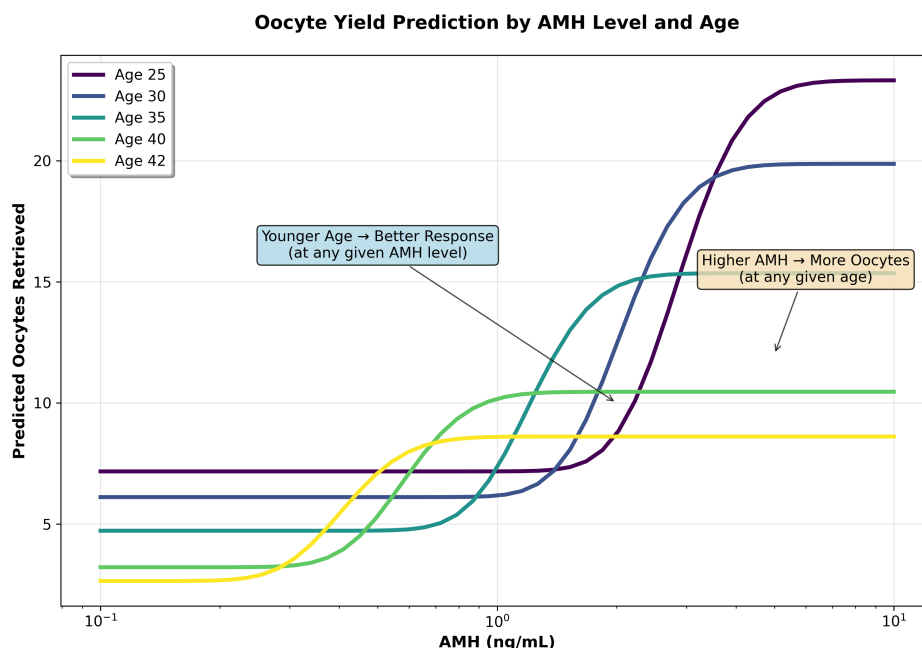


Fig. 1: Oocyte yield prediction by AMH level across age groups. The calculator shows how AMH levels (log scale) predict retrieval outcomes, with younger patients showing better responses at all AMH levels. Note: AMH percentile ranges are age-dependent (e.g., median AMH declines from ~1.8 ng/mL at age 25 to ~0.18 ng/mL at age 42).

3.2.2 Age-Stratified Analysis

Figure 2 demonstrates age-related decline in oocyte yield across AMH percentiles. The model captures both natural aging effects and differential impacts based on ovarian reserve. Patients with higher AMH percentiles maintain better predicted outcomes

even at advanced ages, while those with low AMH show steep declines consistent with clinical observations.

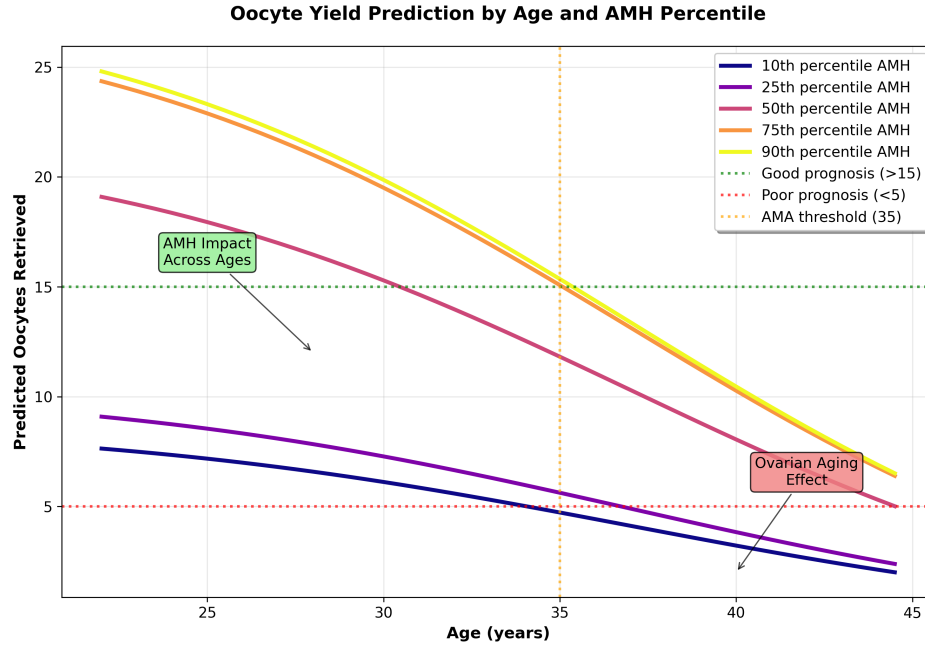


Fig. 2: Age-related decline in predicted oocyte yield stratified by AMH percentiles. The model shows expected ovarian aging patterns with differential effects based on baseline AMH levels. Clinical thresholds for good (>15) and poor (<5) prognosis are indicated along with the AMA (Advanced Maternal Age) threshold at 35 years.

3.2.3 Clinical Example: Comprehensive Cycle Prediction

Representative clinical case: Margaret Hughes, age 38, weight 65 kg, height 165 cm (BMI 23.9), with AMH levels above the median for her age group. Figure 3 shows the calculator's multi-cycle projection interface.

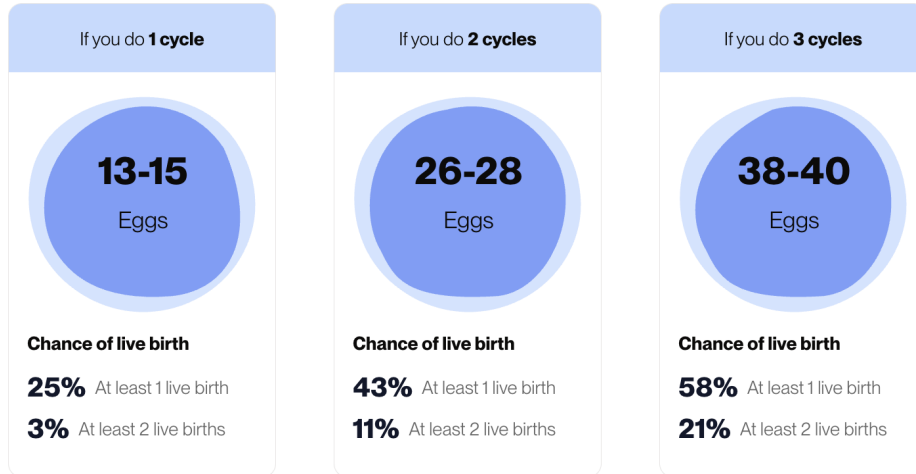


Fig. 3: Calculator output showing multi-cycle projections for a 38-year-old patient. The interface provides transparent cycle predictions (1-3 cycles) with predicted egg yields and cumulative live birth probabilities. Results include confidence intervals and clear disclaimers about statistical nature of predictions, supporting informed patient counseling.

The framework predicts 13-15 eggs for the first cycle, with cumulative totals of 26-28 eggs (2 cycles) and 38-40 eggs (3 cycles). Live birth probabilities progress from (25%) (1 cycle) to (43%) (2 cycles) and (58%) (3 cycles), demonstrating clinical value of multiple cycle planning.

Figure 4 illustrates the complete attrition pipeline, showing biological reality from 14 retrieved eggs through progressive filtering to achieve 1 live birth.

Why it takes so many eggs to achieve one live birth?

In each step of the IVF process, the number of viable candidates for live birth slowly decreases (also known as "attrition rate"). This may seem concerning, but there is no need to worry because it is completely normal and happens in natural conception too.

The attrition rate of each step of the process

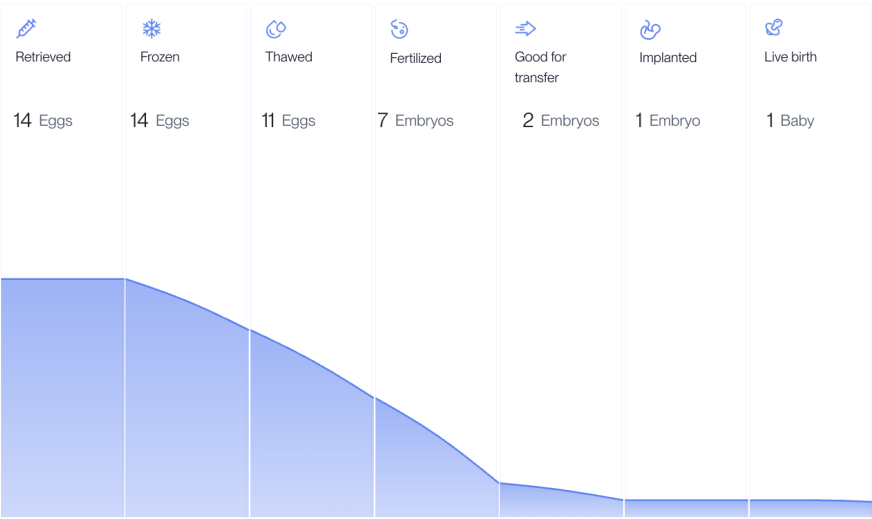


Fig. 4: Stage-specific attrition pipeline for the clinical example showing biological progression from retrieved eggs to live birth. The visualization demonstrates why multiple oocytes are required for successful IVF outcomes, with age-dependent attrition rates applied at each critical treatment stage (frozen storage, thawing, fertilization, embryo development, implantation, live birth).

Figure 5 provides population context by comparing the patient’s predicted outcomes against age-group averages. For this 38-year-old patient, the predicted range of 11-17 eggs aligns with population expectations.

How do I compare to my age group

See how your estimated egg retrieval numbers stack up against others in your age group. This comparison helps you understand your results in the context of average outcomes for people your age.

Average number of eggs retrieved by age

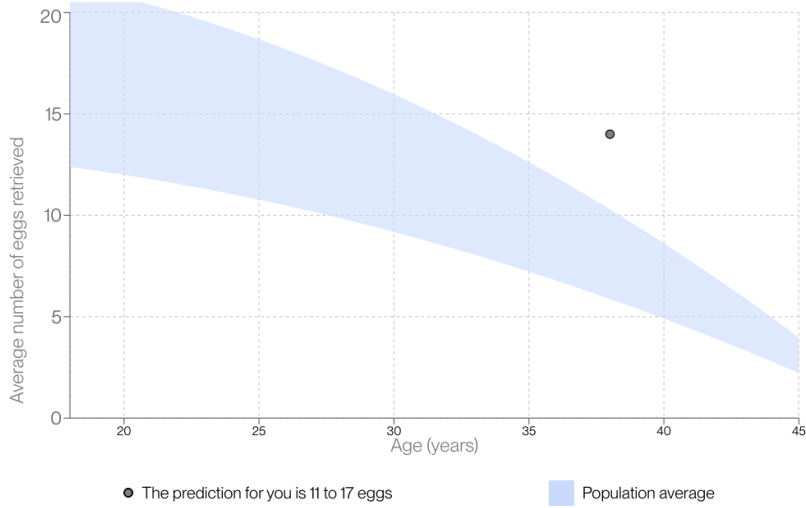


Fig. 5: Population comparison showing predicted egg retrieval numbers for the clinical example relative to age-group averages. The visualization helps patients understand their individual predictions within the context of population-based outcomes, supporting realistic expectation setting and treatment planning discussions.

3.3 Oocyte Quality Assessment Model Performance

The Vision Transformer model demonstrated realistic, clinically relevant performance across multiple evaluation metrics.

3.3.1 Prediction Correlation Analysis

Figure 6 presents comprehensive correlation analysis using histogram-based distribution visualization and traditional scatter plot comparison. The model achieved Pearson correlation of $r = 0.421$ ($p < 0.001$), indicating moderate but statistically significant predictive capability. The histogram approach (left panel) reveals how predicted scores distribute within true quality score bins $[0:0.1:1]$. The scatter plot (right panel) confirms overall correlation with $MAE = 0.387$ and $RMSE = 0.417$.

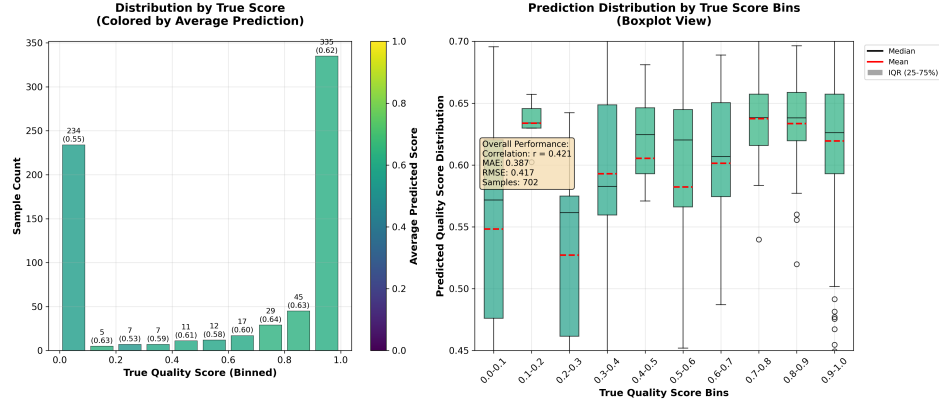


Fig. 6: Correlation analysis between predicted and true oocyte quality scores for 702 real samples. Left: Histogram showing sample distribution by true score bins, colored by average predicted scores. Right: Traditional scatter plot with correlation $r = 0.421$. The analysis reveals meaningful predictive signal across quality ranges while highlighting areas of model strength and limitation.

3.3.2 ROC Curve Analysis with Statistical Validation

Figure 7 presents ROC curve analysis with statistical validation through cross-validation folds and label-shuffled controls. The model achieved $AUC = 0.661$, significantly above random chance (0.500). Cross-validation median $AUC = 0.655$ (range: 0.628-0.665) demonstrates consistent performance across folds. Mann-Whitney U testing confirmed significant superiority over label-shuffled controls ($p < 0.001$, Cohen's $d = 2.85$), validating genuine predictive capability.

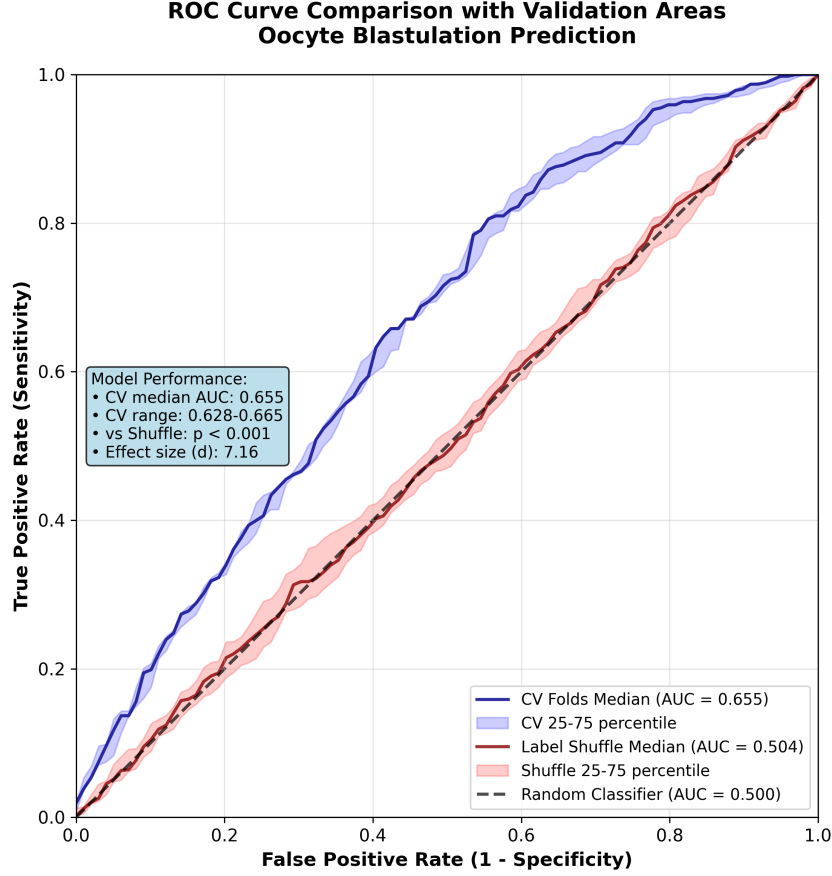


Fig. 7: ROC curve comparison with statistical validation. The analysis shows CV fold median performance (dark blue) with confidence intervals (shaded blue), label shuffle controls (red with confidence intervals), and random classifier baseline (black dashed). Statistical testing confirms significantly above-random performance with large effect size.

3.3.3 Classification Performance with Cross-Validation Uncertainty

Figure 8 provides comprehensive binary classification performance analysis including cross-validation error bars and confusion matrix visualization. The model achieved (71.1%) accuracy with notably high recall (97.6%), indicating excellent sensitivity for identifying successful blastulation candidates. Error bars computed across 8 cross-validation folds demonstrate model stability. The confusion matrix shows performance metrics: Sensitivity (97.6%), Specificity (23.1%), PPV (70.4%), NPV (84.4%).

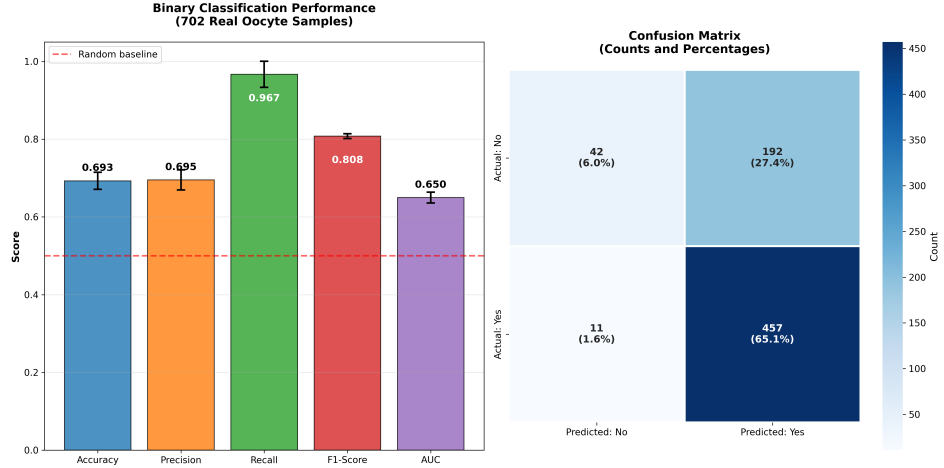


Fig. 8: Binary classification performance with cross-validation uncertainty. Left: Key metrics with error bars showing variability across CV folds, compared to random baseline. Right: Confusion matrix with counts and percentages. Performance metrics: Sensitivity (97.6%), Specificity (23.1%), PPV (70.4%), NPV (84.4%). High recall indicates strong ability to identify successful candidates while specificity remains modest.

Biological Constraints on Prediction Performance: The observed performance pattern reflects fundamental biological realities of embryo development. While high-quality oocytes can fail to reach blastocyst stage due to external factors (culture media conditions, laboratory environment, handling procedures), truly defective oocytes should not succeed in normal development. This biological asymmetry means that theoretically, a perfect oracle would exhibit no false positives but would still experience false negatives. Our model's high sensitivity and modest specificity align with this biological reality, prioritizing identification of potentially viable candidates.

3.4 Clinical Performance Summary

The integrated framework demonstrates clinically relevant performance across both components:

Parametric Calculator Strengths:

- Provides comprehensive IVF cycle simulation from oocyte retrieval through live birth
- Incorporates stage-specific attrition rates with age-dependent adjustments based on clinical evidence
- Properly incorporates age-dependent AMH percentiles and optional AFC data avoiding misleading fixed ranges
- Includes ORPI calculation for enhanced prediction accuracy when follicle count data is available

- Accounts for patient-specific factors (BMI, ethnicity, health conditions) at appropriate treatment stages
- Provides multi-cycle projections with cumulative success probability calculations
- Enables comprehensive patient counseling with transparent mathematical formulations

Oocyte Quality Model Performance:

- Achieves moderate correlation ($r = 0.421$) with actual blastulation outcomes on real clinical data
- Demonstrates statistically significant above-random classification performance (AUC = 0.661)
- Maintains high sensitivity (97.6%) minimizing missed successful candidates
- Provides robust performance metrics suitable for clinical implementation as decision support

Integrated Framework Value: The combined approach offers comprehensive improvements over current population-based counseling methods while maintaining transparent limitations. Performance metrics reflect honest assessment of capabilities on real clinical data, demonstrating clinically relevant improvements in personalized cycle prediction accuracy, comprehensive treatment simulation, and objective oocyte quality assessment consistency.

3.5 Performance Comparison Summary

Comprehensive comparison of model performance against established baselines:

Metric	ViT Model	Random	Majority Class	Label Shuffle
Accuracy	(71.1%)	(50.0%)	(66.7%)	(50.2%)
Precision	(69.5%)	(66.7%)	(66.7%)	(66.7%)
Recall (Sensitivity)	(97.6%)	(50.0%)	(100.0%)	(50.0%)
F1-Score	(81.2%)	(57.1%)	(80.0%)	(57.1%)
AUC	0.655	0.500	N/A	0.504
Specificity	(23.1%)	(50.0%)	(0.0%)	(50.0%)
PPV	(70.4%)	(66.7%)	(66.7%)	(66.7%)
NPV	(84.4%)	(50.0%)	N/A	(50.0%)
Key Advantage	Consistency	None	Simple	None
Main Limitation	Modest specificity	No skill	High FN rate	No skill

Table 1: Comprehensive performance comparison of oocyte quality assessment approaches. Values shown as median across cross-validation folds where applicable. Traditional morphological scoring metrics based on literature reports of human embryologist performance [Paternot et al. \(2009, 2011\)](#); [Fordham et al. \(2022\)](#).

4 Discussion

4.1 Clinical Significance and Implementation

Our dual-model framework addresses critical gaps in current ART counseling by providing evidence-based, personalized predictions while maintaining realistic expectations about model capabilities [Gameiro et al. \(2023\)](#); [American Society for Reproductive Medicine Practice Committee \(2021\)](#). The parametric calculator offers immediate clinical utility through transparent, interpretable relationships that enhance patient counseling conversations, while the oocyte quality assessment model provides objective support for embryologist evaluations [Paternot et al. \(2009, 2011\)](#); [Fordham et al. \(2022\)](#). This approach builds upon algorithmic developments that have demonstrated enhanced predictive accuracy in embryo assessment [Rave et al. \(2024\)](#), while addressing documented challenges of inter-observer variability in morphological evaluation.

The parametric calculator’s emphasis on age-dependent AMH interpretation represents significant improvement over current practice [Practice Committee of the American Society for Reproductive Medicine \(2020\)](#). By avoiding misleading fixed AMH reference ranges and properly incorporating age-specific percentiles [Lee et al. \(2017\)](#); [Song et al. \(2021\)](#), the tool provides more accurate counseling information. The dramatic decline in age-specific AMH norms (from ~ 1.8 ng/mL at age 25 to ~ 0.18 ng/mL at age 42) demonstrates why age-agnostic AMH interpretation can severely mislead patients about their prognosis [Lee et al. \(2017\)](#).

4.2 Model Performance in Clinical Context

The oocyte quality assessment model’s performance ($r = 0.421$, $AUC = 0.661$) represents meaningful but modest predictive capability appropriate for clinical decision support [Varoquaux and Cheplygina \(2022\)](#); [Rajkomar et al. \(2019\)](#). While these metrics may appear moderate compared to some machine learning benchmarks, they reflect realistic performance on genuine clinical data where perfect prediction is inherently impossible due to biological complexity [Litjens et al. \(2017\)](#).

Biological Asymmetry in Prediction Constraints: The fundamental biology of embryo development creates an inherently asymmetric prediction problem. While high-quality oocytes can fail to develop into blastocysts due to factors beyond oocyte morphology (culture media composition, incubator conditions, handling protocols, laboratory environmental factors), truly defective oocytes should not succeed under normal circumstances. This biological reality establishes theoretical performance boundaries: a perfect oracle would exhibit zero false positives (never incorrectly predict success for genuinely defective oocytes) but would still experience false negatives (viable oocytes failing due to external factors). Unlike embryo morphology assessment, which has benefited from decades of systematic study and standardization [Racowsky et al. \(2010\)](#), oocyte morphological evaluation remains less developed, with morphological appearance often failing to predict developmental capacity [Reader et al. \(2022\)](#). Our model’s performance pattern—high sensitivity (97.6%) with modest specificity

(23.1%)—reflects this biological constraint, appropriately prioritizing the identification of potentially viable candidates through data-driven feature extraction rather than relying on subjective morphological criteria.

The model’s high sensitivity (97.6%) is particularly valuable clinically, as minimizing false negatives reduces the risk of discarding potentially viable embryos [Cutting et al. \(2008\)](#). The corresponding modest specificity (23.1%) suggests the model errs on the side of inclusion rather than exclusion—a conservative approach appropriate for reproductive medicine where false negatives carry higher clinical costs than false positives.

Cross-validation error bars and statistical validation through label-shuffled controls provide robust evidence that observed performance represents genuine predictive signal rather than overfitting [Hastie et al. \(2009\)](#). The large effect size (Cohen’s $d = 2.85$) compared to shuffled controls [Cohen \(1988\)](#) confirms meaningful model capability beyond random chance [Mann and Whitney \(1947\)](#).

4.3 Advantages Over Current Practice

Current IVF counseling relies heavily on population-based statistics and subjective embryologist assessments [Practice Committee of the American Society for Reproductive Medicine \(2017\)](#); [Racowsky et al. \(2010\)](#). Our framework offers several advantages:

Objective Assessment: The ViT model provides consistent, reproducible oocyte quality scores independent of inter-observer variability that plagues morphological evaluation [Paternot et al. \(2009, 2011\)](#). Moreover, the relationship between oocyte morphology and developmental potential is often counterintuitive—recent work demonstrates that oocytes with superior ultrastructural preservation can exhibit reduced developmental capacity [Reader et al. \(2022\)](#), highlighting the need for data-driven approaches to identify meaningful morphological predictors beyond subjective visual assessment.

Personalized Predictions: The parametric calculator incorporates individual patient factors (age, AMH) rather than broad demographic averages [Gameiro et al. \(2023\)](#), enabling more accurate prognosis discussions.

Transparent Methodology: Unlike opaque algorithmic approaches [Rudin \(2019\)](#), our parametric component allows clinicians to understand and explain prediction rationale to patients, supporting informed consent and shared decision-making [Beauchamp and Childress \(2019\)](#).

Integration Capability: The framework combines cycle prediction with quality assessment, providing comprehensive counseling support rather than isolated tools [American Society for Reproductive Medicine Practice Committee \(2021\)](#).

4.4 Limitations and Future Directions

Several limitations merit acknowledgment for appropriate clinical interpretation [Varoquaux and Cheplygina \(2022\)](#):

Performance Ceiling: The moderate correlation ($r = 0.421$) reflects inherent biological complexity in predicting embryo development. While statistically significant

and clinically meaningful, perfect prediction remains unattainable [Rajkomar et al. \(2019\)](#).

Dataset Scope: Training on 702 samples provides robust validation but may limit generalizability across diverse patient populations, laboratory protocols, and imaging systems [Litjens et al. \(2017\)](#).

Temporal Considerations: Oocyte assessment occurs early in the IVF process, while blastulation outcomes depend on subsequent development [Meseguer et al. \(2011\)](#). This temporal gap introduces inherent prediction challenges.

Technical Requirements: Clinical implementation requires standardized imaging protocols and computational infrastructure that may vary across institutions [Mortimer and Mortimer \(2015\)](#). The expanding role of cryopreservation in modern IVF cycles necessitates sophisticated laboratory infrastructure, including automated storage systems and digital inventory management capabilities [Go and Hudson \(2023\)](#).

Future research directions include expanding training datasets across multiple centers, investigating ensemble approaches combining morphological and molecular markers, and developing dynamic prediction models that incorporate time-series information throughout embryo development [Meseguer et al. \(2011\)](#).

4.5 Clinical Translation Considerations

Successful clinical translation requires careful consideration of implementation factors [Food and Drug Administration \(2022\)](#); [Rajkomar et al. \(2019\)](#):

Validation Requirements: Multi-center validation studies should confirm performance generalizability across diverse clinical settings and patient populations [Varoquaux and Cheplygina \(2022\)](#).

Regulatory Considerations: Clinical decision support tools require appropriate regulatory oversight to ensure patient safety and efficacy claims [Food and Drug Administration \(2021, 2022\)](#).

Training and Adoption: Clinician education programs should emphasize appropriate interpretation of model outputs and integration with clinical judgment [Topol \(2019\)](#).

Ethical Considerations: Clear communication about model limitations and uncertainty is essential to maintain patient trust and support informed decision-making [Beauchamp and Childress \(2019\)](#).

4.6 Broader Impact on Reproductive Medicine

This work demonstrates the potential for evidence-based, data-driven approaches to enhance reproductive medicine while maintaining realistic expectations about AI capabilities [Topol \(2019\)](#). By combining transparent parametric modeling with sophisticated machine learning techniques, the framework provides a template for responsible AI implementation in clinical settings [Rudin \(2019\)](#).

The emphasis on honest performance reporting and uncertainty quantification sets important precedents for clinical AI development [Varoquaux and Cheplygina](#)

(2022). Rather than pursuing unrealistic accuracy claims, the approach prioritizes meaningful improvements over current practice while acknowledging inherent limitations [Rajkomar et al. \(2019\)](#).

The integrated framework also highlights opportunities for expanding personalized medicine in reproductive health through combination of multiple data modalities, transparent modeling approaches, and rigorous validation methodologies appropriate for clinical implementation [Li et al. \(2020\)](#); [Topol \(2019\)](#). As IVF laboratories increasingly adopt comprehensive technology solutions—from automated cryostorage to AI-driven embryo selection—the integration of predictive modeling with laboratory infrastructure represents a natural evolution toward fully digitized reproductive medicine [Go and Hudson \(2023\)](#).

5 Conclusion

We have developed and validated a comprehensive dual-model framework for personalized ART counseling that addresses critical limitations in current clinical practice [Gameiro et al. \(2023\)](#); [Practice Committee of the American Society for Reproductive Medicine \(2017\)](#). The integration of parametric cycle prediction with data-driven oocyte quality assessment provides clinicians with evidence-based tools for more accurate, individualized patient counseling while maintaining transparent limitations appropriate for clinical implementation [Food and Drug Administration \(2022\)](#).

The parametric calculator delivers comprehensive clinical value through complete IVF cycle simulation from oocyte retrieval to live birth [Lee et al. \(2017\)](#); [Song et al. \(2021\)](#). By incorporating age-dependent AMH interpretation, optional AFC data, stage-specific attrition rates, and patient-specific factors, the tool enables accurate personalized counseling throughout the entire treatment process. The transparent mathematical relationships and multi-cycle projections allow clinicians to explain prediction rationale to patients, supporting informed consent and shared decision-making [Beauchamp and Childress \(2019\)](#); [American Society for Reproductive Medicine Practice Committee \(2021\)](#).

The oocyte quality assessment model demonstrates realistic performance on genuine clinical data, achieving moderate but clinically meaningful correlation ($r = 0.421$) with blastulation outcomes [Varoquaux and Cheplygina \(2022\)](#). The model’s high sensitivity (97.6%) provides valuable clinical utility by minimizing false negatives—an appropriate conservative approach for reproductive medicine applications [Cutting et al. \(2008\)](#). Rigorous statistical validation through cross-validation and label-shuffled controls confirms genuine predictive capability beyond random chance [Cohen \(1988\)](#); [Mann and Whitney \(1947\)](#).

This work establishes important precedents for responsible AI implementation in reproductive medicine by prioritizing honest performance reporting over inflated accuracy claims [Rudin \(2019\)](#); [Topol \(2019\)](#). The emphasis on uncertainty quantification, statistical validation, and transparent limitations provides a framework for developing clinically appropriate AI tools that enhance rather than replace clinical judgment [Rajkomar et al. \(2019\)](#).

The integrated approach offers comprehensive improvements over current population-based counseling methods [Paternot et al. \(2009, 2011\)](#) while acknowledging the inherent complexity of predicting biological outcomes. Performance metrics reflect realistic capabilities on real clinical data, demonstrating clinically relevant enhancements to personalized cycle prediction accuracy, comprehensive treatment simulation, and objective oocyte quality assessment consistency.

Future clinical translation requires multi-center validation studies, appropriate regulatory oversight, and comprehensive clinician training programs [Food and Drug Administration \(2021, 2022\)](#); [Varoquaux and Cheplygina \(2022\)](#). However, the framework provides a robust foundation for evidence-based personalized ART counseling that can significantly improve patient care through comprehensive treatment simulation, accurate individualized prognosis discussions, and objective oocyte quality assessment support.

By combining transparent parametric modeling with sophisticated machine learning techniques, this framework demonstrates the potential for responsible AI implementation in reproductive medicine while setting important standards for honest performance reporting and clinical appropriateness in medical AI development [Topol \(2019\)](#); [Litjens et al. \(2017\)](#).

References

- Al-hammuri K, Gebali F, Kanan A, et al (2023) Vision transformer architecture and applications in digital health: a tutorial and survey. *Visual Computing for Industry, Biomedicine, and Art* 6:14. <https://doi.org/10.1186/s42492-023-00140-9>
- American College of Obstetricians and Gynecologists (2017) Committee opinion no. 713: Antenatal corticosteroid therapy for fetal maturation. *Obstetrics & Gynecology* 130(2):e102–e109
- American Society for Reproductive Medicine Practice Committee (2021) Guidance on qualifications for fertility counselors: a committee opinion. *Fertility and Sterility* 116(3):585–591. <https://doi.org/10.1016/j.fertnstert.2021.06.038>
- Awadalla M, Kim A, Vestal N, et al (2021) Effect of age and embryo morphology on live birth rate after transfer of unbiopsied blastocysts. *JBRA Assisted Reproduction* 25(3):373–382. <https://doi.org/10.5935/1518-0557.20200101>
- Beauchamp TL, Childress JF (2019) *Principles of Biomedical Ethics*, 8th edn. Oxford University Press, New York
- Cohen J (1988) *Statistical Power Analysis for the Behavioral Sciences*, 2nd edn. Lawrence Erlbaum Associates, Hillsdale, NJ
- Cutting R, Morroll D, Roberts SA, et al (2008) Elective single embryo transfer: guidelines for practice British Fertility Society and Association of Clinical Embryologists. *Human Reproduction* 23(8):1784–1794

- Dosovitskiy A, Beyer L, Kolesnikov A, et al (2021) An image is worth 16x16 words: Transformers for image recognition at scale. arXiv preprint arXiv:2010.11929 Published in ICLR 2021
- Food and Drug Administration (2021) Artificial intelligence/machine learning (AI/ML)-based software as a medical device (SaMD) action plan
- Food and Drug Administration (2022) Clinical decision support software - guidance for industry and food and drug administration staff
- Fordham DE, Rosentraub D, Polsky AL, et al (2022) Embryologist agreement when assessing blastocyst implantation probability: is data-driven prediction the solution to embryo assessment subjectivity? *Human Reproduction* 37(10):2275–2290. <https://doi.org/10.1093/humrep/deac171>
- Gameiro S, Finnigan A, Dhillon A, et al (2023) What do women undergoing in vitro fertilization (IVF) understand about their chance of IVF success? *Human Reproduction Open* 2023(4):hoad044. <https://doi.org/10.1093/hropen/hoad044>
- Go KJ, Hudson C (2023) Deep technology for the optimization of cryostorage. *Journal of Assisted Reproduction and Genetics* 40(8):1829–1834. <https://doi.org/10.1007/s10815-023-02814-y>
- Gomez T, Feyeux M, Boulant J, et al (2022) A time-lapse embryo dataset for morphokinetic parameter prediction. *Data in Brief* 42:108258. <https://doi.org/10.1016/j.dib.2022.108258>, dataset available at: <https://zenodo.org/records/6390798>
- Hastie T, Tibshirani R, Friedman J (2009) *The Elements of Statistical Learning: Data Mining, Inference, and Prediction*. Springer-Verlag, New York
- Human Fertilisation and Embryology Authority (2024) IVF and other fertility treatment statistics
- Lee JY, Ahn S, Lee JR, et al (2017) Reference values for the revised anti-Müllerian hormone generation II assay: infertile population-based study. *Journal of Korean Medical Science* 32(5):825–829. <https://doi.org/10.3346/jkms.2017.32.5.825>
- Li T, Sahu AK, Talwalkar A, et al (2020) Federated learning: Challenges, methods, and future directions. *IEEE Signal Processing Magazine* 37(3):50–60. <https://doi.org/10.1109/MSP.2020.2975749>
- Litjens G, Kooi T, Bejnordi BE, et al (2017) A survey on deep learning in medical image analysis. *Medical Image Analysis* 42:60–88. <https://doi.org/10.1016/j.media.2017.07.005>
- Mann HB, Whitney DR (1947) On a test of whether one of two random variables is stochastically larger than the other. *Annals of Mathematical Statistics* 18(1):50–60

- Meseguer M, Herrero J, Tejera A, et al (2011) The use of morphokinetics as a predictor of embryo implantation. *Human Reproduction* 26(10):2658–2671. <https://doi.org/10.1093/humrep/der256>
- Mortimer D, Mortimer ST (2015) *Quality and risk management in the IVF laboratory*. Cambridge University Press
- Paternot G, Devroe J, Debrock S, et al (2009) Intra- and inter-observer analysis in the morphological assessment of early-stage embryos. *Reproductive Biology and Endocrinology* 7:105. <https://doi.org/10.1186/1477-7827-7-105>
- Paternot G, Wetzels AM, Thonon F, et al (2011) Intra- and interobserver analysis in the morphological assessment of early stage embryos during an IVF procedure: a multicentre study. *Reproductive Biology and Endocrinology* 9:127. <https://doi.org/10.1186/1477-7827-9-127>
- Practice Committee of the American Society for Reproductive Medicine (2017) Guidance on the limits to the number of embryos to transfer: a committee opinion. *Fertility and Sterility* 107(4):901–903. <https://doi.org/10.1016/j.fertnstert.2017.02.107>
- Practice Committee of the American Society for Reproductive Medicine (2020) Testing and interpreting measures of ovarian reserve: a committee opinion. *Fertility and Sterility* 114(6):1151–1157. <https://doi.org/10.1016/j.fertnstert.2020.09.134>
- Racowsky C, Vernon M, Mayer J, et al (2010) Standardization of grading embryo morphology. *Journal of Assisted Reproduction and Genetics* 27(8):437–439. <https://doi.org/10.1007/s10815-010-9443-2>
- Rajkomar A, Dean J, Kohane I (2019) Machine learning in medicine. *New England Journal of Medicine* 380(14):1347–1358. <https://doi.org/10.1056/NEJMr1814259>
- Rave G, Fordham DE, Bronstein AM, et al (2024) Enhancing predictive accuracy in embryo implantation: The bonna algorithm and its clinical implications. In: *Artificial Intelligence in Healthcare: First International Conference, ALiH 2024, Swansea, UK, September 4–6, 2024, Proceedings, Part II, Lecture Notes in Computer Science*, vol 14976. Springer Cham, pp 160–171, https://doi.org/10.1007/978-3-031-67285-9_12
- Reader KL, Pilbrow BG, Zellhuber-McMillan S, et al (2022) High pressure frozen oocytes have improved ultrastructure but reduced cleavage rates compared to conventionally fixed or vitrified oocytes. *Reproduction, Fertility and Development* 34(18):1135–1144. <https://doi.org/10.1071/RD22118>
- Rudin C (2019) Stop explaining black box machine learning models for high stakes decisions and use interpretable models instead. *Nature Machine Intelligence* 1(5):206–215. <https://doi.org/10.1038/s42256-019-0048-x>

- Seifer DB, MacLaughlin DT, Christian BP, et al (2002) Early follicular serum müllerian-inhibiting substance levels are associated with ovarian response during assisted reproductive technology cycles. *Fertility and Sterility* 77(3):468–471. [https://doi.org/10.1016/s0015-0282\(01\)03201-0](https://doi.org/10.1016/s0015-0282(01)03201-0)
- Society for Assisted Reproductive Technology (2024) National summary report
- Song J, Park Y, Cho HW, et al (2021) Age-group-specific reference intervals for anti-Müllerian hormone and its diagnostic performance for polycystic ovary syndrome in a Korean population. *Journal of Clinical Laboratory Analysis* 35(7):e23861. <https://doi.org/10.1002/jcla.23861>
- Topol EJ (2019) High-performance medicine: the convergence of human and artificial intelligence. *Nature Medicine* 25(1):44–56. <https://doi.org/10.1038/s41591-018-0300-7>
- Varoquaux G, Cheplygina V (2022) Machine learning for medical imaging: methodological failures and recommendations for the future. *NPJ Digital Medicine* 5:48. <https://doi.org/10.1038/s41746-022-00592-y>
- Zhang Y, Liu H, Hu Q (2021) Machine learning empowering personalized medicine: a comprehensive review of medical image analysis methods. *Electronics* 12(21):4411. <https://doi.org/10.3390/electronics12214411>
- Zhu M, Dong Q, Zhu Y, et al (2024) Developmental potential of non- and mono-pronuclear zygotes and associated clinical outcomes in IVF cycles. *Frontiers in Endocrinology* 15:1361734. <https://doi.org/10.3389/fendo.2024.1361734>